



Machine learning approach to the detection of point sources in maps of the CMB temperature anisotropies

P. Diego-Palazuelos^{1,2}, R. B. Barreiro¹, P. Vielva¹, D. Balbás³, M. López-Caniego⁴,
D. Herranz^{1,2}, and B. Casaponsa¹

- ¹ Instituto de Física de Cantabria (CSIC-UC), Santander, Spain
² Departamento de Física Moderna, Universidad de Cantabria, Santander, Spain
³ IMDEA Software Institute, Madrid, Spain
⁴ Aurora Technology for the European Space Agency, Madrid, Spain
e-mail: diegop@ifca.unican.es

Received: 17-10-2022; Accepted: 21-02-2023

Abstract. We propose a machine learning approach to the blind detection of extragalactic point sources on maps of the temperature anisotropies of the cosmic microwave background. Using realistic simulations of the microwave sky as seen by *Planck*, we train a convolutional neural network (CNN) that solves source detection as an image segmentation problem. We divide the sky into regions of progressively increasing Galactic foreground intensity and independently train specialized CNNs for each region. This strategy leads to promising levels of completeness and reliability, with our CNN substantially outperforming traditional detection methods like the matched filter in regions close to the Galactic plane.

Key words. Cosmic Microwave Background – Point Source Detection – Convolutional Neural Networks – Image Segmentation

1. Introduction

To extract cosmological information from cosmic microwave background (CMB) observations, we must first separate its signal from the rest of Galactic and extragalactic emissions (Delabrouille & Cardoso , 2007). Therefore, although they are an interesting subject of study on their own (de Zotti et al. , 2018), extragalactic sources emitting in the microwave range (e.g., radio-loud active galactic nuclei or dusty galaxies) constitute a contaminant that must be removed to extract infor-

mation from the small angular scales of CMB data (Tucci et al. , 2005).

Traditionally, algorithms for the detection of compact sources have combined wavelet or linear filters defined to maximize the signal-to-noise ratio of sources with respect to the background with a thresholding detection criterion (Herranz & Vielva , 2010). As an alternative, we propose a machine learning approach to the blind detection of extragalactic point sources on maps of the temperature anisotropies of the CMB. We treat source detection as an image segmentation problem and

design a convolutional neural network (CNN) that successfully solves it while maintaining a simple autoencoder architecture. Note that with this approach we are decoupling the process of source localization from flux estimation. As it does not need to reconstruct the flux of sources, our CNN can detect sources down to lower fluxes and immersed in more complex astrophysical backgrounds than algorithms based on unbiased flux estimators like the matched filter (MF) (López-Caniego et al., 2006).

2. Methodology

We train and test our CNN using realistic simulations of the microwave sky as seen by the 143 GHz frequency band of the *Planck* mission (*Planck* Collaboration I, 2020). These mock observations contain CMB realizations according to *Planck*'s best-fit cosmological model (*Planck* Collaboration VI, 2020), realistic simulations of instrumental noise (*Planck* Collaboration I, 2020), and Galactic and extragalactic foregrounds. We use the *Planck Sky Model*¹ (Delabrouille et al., 2020) to simulate the synchrotron, thermal dust, spinning dust, and free-free diffuse Galactic emissions, and the extragalactic thermal and kinetic Sunyaev-Zeldovich effects. We generate extragalactic point sources following the number counts per flux density models of Tucci et al. (2011). Taking the *Planck* Collaboration XXVI (2016) catalog as reference, we distinguish between detectable (labeled) sources and a background of faint undetectable (unlabeled) sources with fluxes below 177 mJy.

We project the sky into two-dimensional $3.63^\circ \times 3.63^\circ$ patches and, based on their mean Galactic foreground intensity, divide them into partially overlapping regions of faint, medium, and bright foreground emission. These regions approximately cover a 65%, 40%, and 25% fraction of the sky, respectively. Inside each region, patches are separated into alternating rings of equal longitude to evenly divided them into training and validation sets that do not overlap between them.

¹ <https://pla.esac.esa.int>

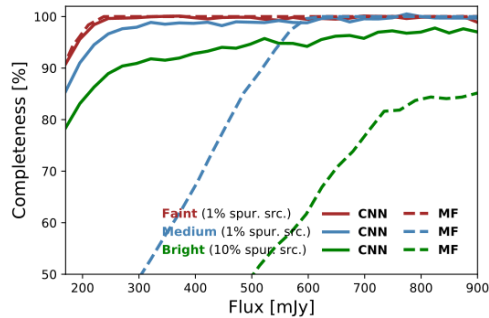


Fig. 1. Percentage of detected sources above a given flux using the MF (dashed) and our CNN (solid). Results are shown for the regions of faint (red), medium (blue), and bright (green) Galactic foreground emission, indicating the percentage of spurious detections allowed in each case.

We use supervised learning with binary labels to train independent CNNs that specialize in each region. However, the higher complexity of foregrounds and the reduced size of the training sample lead to over-fitting on the region of brightest foreground emission. Preliminary results show that the generalization ability of the CNN trained for bright foreground emission improves when increasing the size of the training set with rotated and rescaled patches from other regions of the sky and applying regularization techniques such as dropout (Tompson et al., 2015). After implementing these procedures, the results presented in Section 3 do not show any significant signs of over-fitting.

3. Results

In Figure 1, we show the preliminary results that we obtain when applying the CNN to the validation set defined in Section 2 and compare them with those obtained using traditional methods like the MF. Both methods perform similarly well in regions far from the Galactic plane where the CMB dominates over the foreground emission (red lines).

Once we move to regions of the sky dominated by Galactic emission, the MF is outperformed by the CNN as it is no longer able to characterize the statistics of the background.

Compared to the MF, our CNN reduces the flux at which a 90% completeness is reached from 514 mJy to 195 mJy (1% of spurious detections allowed) in the region of intermediate foreground intensity (blue lines). It is inside the Galactic plane (green lines) where our CNN would provide a substantial improvement on the completeness of current catalogs, achieving a 90% completeness at 270 mJy while yielding only a 10% of spurious detections. Under the same conditions, the flux threshold of the MF is at 1013 mJy.

4. Conclusions and future work

Although dropout and data augmentation can satisfactorily solve our over-fitting problem, we would like to further improve the robustness of our CNN by exploring different options. E.g., increasing the number of training samples for all regions by reducing the size of patches, or applying transfer learning (A. Farahani et al., 2021) to progressively specialize the CNN towards regions of brighter foreground emission instead of training independent CNNs for each region.

Once over-fitting is fully under control, we will be ready to extend the training to other frequencies. Our preliminary results lead us to believe that, once applied to data, the CNN will produce deeper and more complete catalogs of extragalactic sources.

Acknowledgements. PDP, RBB, PV, and DH acknowledge funding from the Unidad de Excelencia

María de Maeztu (MDM-2017-0765). PDP, RBB, and PV thank the Spanish Agencia Estatal de Investigación (AEI, MICIU) for the financial support provided under the project PID2019-110610RB-C21, and DH for that under the project PGC2018-101814-B-I00. PDP also acknowledges funding from the *Formación del Profesorado Universitario* program of the Spanish Ministerio de Ciencia, Innovación y Universidades. We acknowledge the use of the *Planck Sky Model*, TensorFlow, Keras, HEALPix, Scipy, skimage, Matplotlib, and NumPy.

References

- J. Delabrouille & J. F. Cardoso, arXiv eprints [astro-ph/0702198] (2007)
- J. Delabrouille et al., *A&A*, 553, A96 (2013)
- A. Farahani et al., arXiv eprints [2104.02144] (2021)
- D. Herranz & P. Vielva, *IEEE Signal Process. Mag.*, 27(1), 67 (2010)
- M. López-Cañiego et al., *MNRAS*, 370(4) 2047 (2006)
- Planck* Collaboration I, *A&A*, 641, A1 (2020)
- Planck* Collaboration VI, *A&A*, 641, A6 (2020)
- Planck* Collaboration XXVI, *A&A*, 594, A26 (2016)
- J. Tompson et al., *Proc. 2015 IEEE Comput. Soc. Conf. Comput. Vis. Pattern Recognit.*, 648 (2015)
- M. Tucci et al., *MNRAS*, 360(3) 935 (2005)
- M. Tucci et al., *A&A*, 533, A57 (2011)
- G. de Zotti et al., *JCAP*04(2018)020 (2018)